Journal of
NANOSTRUCTURES
JNS
NANOSTRUCTURES
JNS.kashanu.ac.ir

High Solid Contents Copoly (Styrene/Butyl Acrylate)-Cloisite 30B Nanocomposites

M. Mirzataheri

Iran Polymer & Petrochemical Institute, P. O. Box. 14965/115, Tehran, Iran

Article history:
Received 24/2/2013
Accepted 11/5/2013
Published online 1/6/2013

Keywords:
High solid content
Latex
Nanoclay
Nanocomposite

**Corresponding author:*
E-mail address*:*
m.mirzataheri@ippi.ac.ir
Phone: 98 912 1893 880
Fax: +98 21 44580023

Abstract

Higher solid contents (20 % and 40 %) nanocomposites of poly (styrene-co-butyl acrylate) including higher content of Cloisite 30B (7 wt% and 10 wt %) were prepared via miniemulsion polymerization. Stability of the final latexes proved outstanding combination of polymerization procedure and surfactants. Morphological studies revealed by TEM, SAX and XRD showed three structures of core-shell, armored and individual dispersion of clay layers within the polymer particles. The effect of Cloisite 30B content on the barrier properties presents excellent and wide use of these films for packaging and nanocoatings industries.

1. Introduction

The first polymer/clay nanocomposite was reported by Blumstein in 1961 [1-3]. Production of polymer/clay nanocomposite increased when outstanding mechanical and thermal properties of the nylon-6/clay nanocomposite was recorded by the Toyota Research Laboratories Centre in 1993 [4-5]. Clay platelets (with high aspect ratio) can be well dispersed in the polymer matrix and exhibit unique physical and especially barrier properties when apply as coating materials while improve the barrier properties without changing the other properties (Fig. 1).

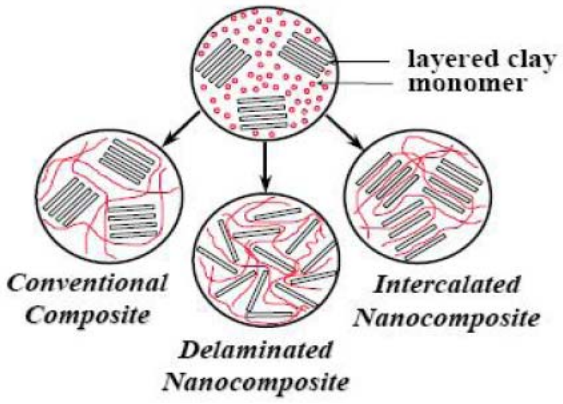

Fig. 1. Three configurations of polymer/clay composites [4].

Dispersion of impermeable clay layers within a polymer/clay nanocomposite has been shown in

Fig. 2 while w is the layer's thickness and L is layer's length. This configuration prepares a tortuous way for permeation of penetrate molecules across the nanocomposite.

Polymer nanocomposites with fully exfoliated structures exhibit excellent barrier properties against gases, water and even, hydrocarbons. Researchers proved that such reduction in permeability definitely depends on the clay aspect ratio, surface area and especially on the degree of intercalation and exfoliation of clay platelets in polymer matrix [6].

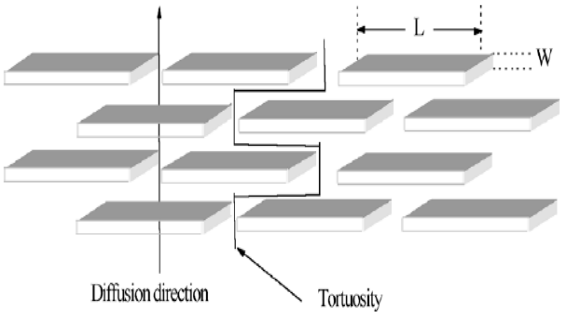

Fig. 2. Diffusion path through the nanocomposite [6].

The best barrier property was obtained in polymer nanocomposites with fully exfoliated clay structures. For polyimide filled with 2 wt% of organoclay, the permeability coefficient decreased greatly [7]. Permeability to water vapor for exfoliated polycaprolactone nanocomposites has also been investigated and indicated a decrease of permeability with increase in the number of exfoliated clay platelets [8].

Miniemulsion is a new method for synthesizing stable emulsion of small droplets, in which monomer droplets are stabilized against Ostwald ripening and coalescence as is shown in Fig. 3. By adding an ultrahydrophobe, the stability against Ostwald ripening can be increased via an additional osmotic pressure [9]. Vigorous mechanical agitation provides the colloidal stability of monomer droplets [9].

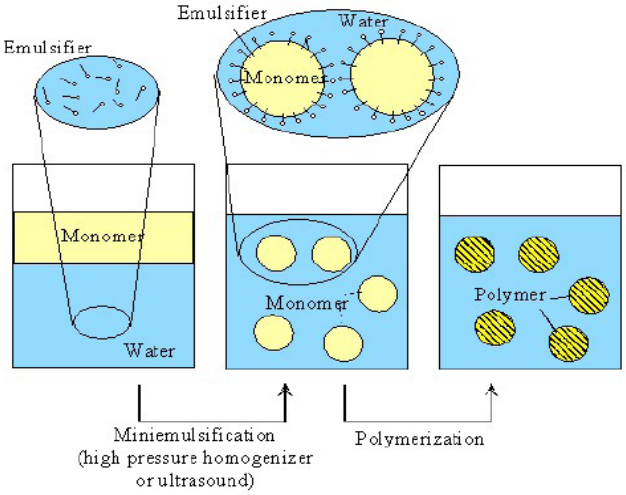

Fig. 3. Principle of miniemulsion procedure [9].

Preparation of miniemulsion for encapsulation purposes consists of two steps (Fig. 4). First, the inorganic material must be dispersed in monomer phase. Hydrophilic pigments require a hydrophobic surface to be well dispersed into the hydrophobic monomer phase which is usually done by a surfactant system 1 with low hydrophilic-lipophilic balance (HLB) value. Then this mixture is emulsified in the water phase, employing a surfactant system 2 with higher HLB, which has a higher tendency to stabilize the monomer or polymer interfaces with water [10].

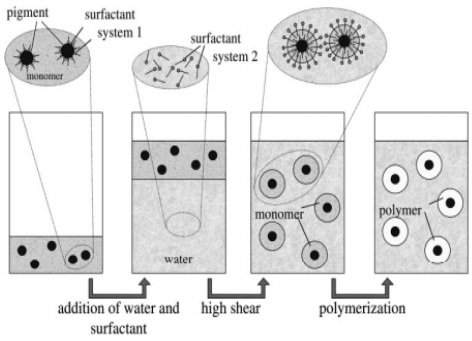

Fig. 4. Encapsulation of pigment by miniemulsion [10].

A liquid which after applying and drying onto a surface appears as a continuous film is named surface coating. Drying is carried out by evaporation or curing. Binder (polymer or resin) is the main component of the coating and forms the continuous film by adhering to the coating substrate and holds the ingredients (such as fillers and pigments) in the film. Based on the compositions, three categories of coatings can be distinguished: water-borne, solvent-borne, and solvent-free [11-14]: Film formation from water-borne polymer latex is schematically drawn in Fig. 5.

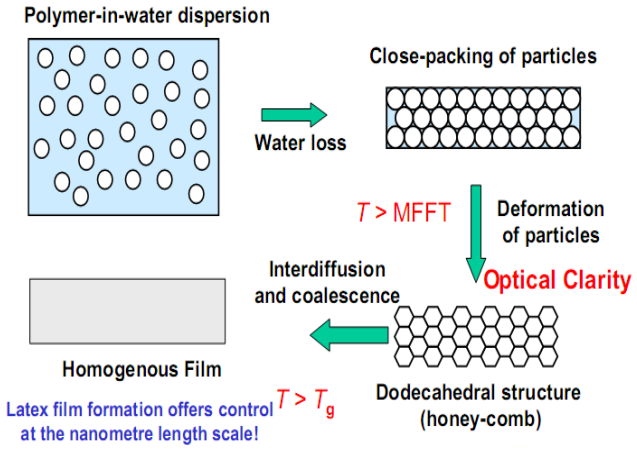

Fig. 5. Film formation from polymer latex [14].

Dungen and coworkers used Pickering miniemulsion of (styrene-co-butyl acrylate) and believed their latexes were more stable than SDS stabilized latexes [15].

Bonnefond and colleagues reported surfactant-free emulsion and miniemulsion polymerizations of styrene and butyl acrylate in presence of Na^+ MMT clay modified with a macromonomer. They decreased the water uptake and water vapor transition rates of polymer [16].

Others explained based on surface hydrophobicity of Cloisite, less hydrophobic compounds can stabilize O/W emulsions, as hydrophobic modified particles act as stabilizer for W/O emulsions [17].

Also it was noted that armored structures for particles covered with the clay platelets can act as super-heat barrier and increase the thermal stability of polymers [18].

Polymer/clay nanocomposite latexes in the form of positively charged nanoparticles were synthesized by activators, in atom transfer radical polymerization (ATRP) of styrene and butyl acrylate in a miniemulsion system [19].

Poly (styrene-co-butyl acrylate) nanocomposite latexes were synthesized via reverse atom transfer radical polymerization (RATRP) in miniemulsion, by using 4,4'-dinonyl-2,2'-bipyridine and a cationic surfactant of cetyltrimethylammonium bromide [20].

In our previous research, poly (styrene-co-butyl acrylate) nanocomposite latex was synthesized with low solid contents (up to 20%) and low clay concentration (up to 5 wt %). By increasing these values, huge coagulation and therefore latex instability was occurred. Also combination of surfactants was needed in order to receive encapsulated structures of about 70 % without any reasonable armored structures [21].

In this research work miniemulsion polymerization was used for making nanocomposites of higher solid contents (20 and 40%) for water-borne poly (styrene-co-butyl acrylate) including higher contents Cloisite 30B (7 wt% and 10 wt%).

For comparison, it should be emphasized that although our results deals with higher clay and higher solid contents, fortunately, all water borne latexes were stable for a long period of time. No instability, coagulation or coalescence was observed. Also by morphological studies was shown that core-shell plus Pickering structures were formed. Therefore, it is possible to control the nanoparticle morphologies just by simple miniemulsion polymerization, without using more chemical reagents, as no one has reported yet. Effect of high

clay concentration and solid content on final properties of nanocomposites such as water absorbency, WVTR and OTR were also investigated and showed distinguished improvements, as we report them here.

2. Experimental procedure

2.1. Materials

Styrene was purified by two times washing with 5% aqueous NaOH solution (W/V) and rinsed with distilled water (until pH of the separated aqueous phase was reached to 7.0). It was stored on dried $CaCl_2$ at 0 °C prior to use. 2, 2′-Azo-bis-isobutyronitrile (AIBN) was kept refrigerated prior to use. All other reagents were analytical grade and were used as received. Cloisite 30B, which is a natural montmorillonite modified with an organic modifier named, methyl tallow bis-2-hydroxyethyl, quaternary ammonium chloride (MT2EtOH), was purchased from Southern Clay Products Company (Gonzales, USA), with d_{001} equal to 1.74.

2.2. Synthesis of copoly (styrene/ butyl acrylate)-Cloisite 30B nanocomposites

Styrene, butyl acrylate, hexadecane, and Span 80 were under magnetic stirring (300 rpm) for 60 min at room temperature and kept cool for 15 min. Then it was placed in sonicator for 10 min. Meanwhile, aqueous phase II was prepared of distilled water and Span 80 under simple stirring at room temperature for 15 min and then kept cool for 15 min. Phase I and phase II were mixed under magnetic stirring for 15 min.

Then, SDS was added to the above dispersion, and further homogenization and ultrasonication was applied by the sonicator probe for 4 min. The prepared miniemulsion with solids content of 20% and 40 % including 7 and 10 wt% clay was used for subsequent polymerization (Table 1). In a four-necked 250 mm glass reactor equipped with condenser, AIBN (1.5 wt% relative to the weight of all monomers) was added and degassed by N_2 at room temperature for 20 min.

Then, the set-up was placed in a water bath at 60 °C and the temperature was kept constant during polymerization reaction. Polymerization was continued at this temperature for 360 min under mechanical stirring (300 rpm) in the presence of sodium bicarbonate (1 wt% relative to the weight of clay and monomers) as buffer.

Finally, reaction was terminated by adding one drop of 1% (W/V) hydroquinone solution in methanol into the latex sample.

It was expected to receive random copolymer of styrene/ butyl acrylate with mostly acrylate end-tethered polymer chains (due to monomer reactivity ratios) surrounded by clay layers. This kind of structure is so demanded for adhesive and coating production [21].

Table 1. Miniemulsion recipe of poly (styrene-co-butyl crylate)-Cloisite 30B nanocomposite latex.

Phases	Components (g)	(20% S.C. &7 wt% Clay)	(20% S.C. &10 wt% Clay)	(40% S.C. &7 wt% Clay)	(40% S.C. &10 wt% Clay)
Phase I	Styrene	12.52	12.19	25.04	24.36
	Butyl acrylate	6.17	6.00	12.34	11.00
	Cloisite 30B	1.31	1.8	2.62	3.64
	Hexadecane	1.12	1.10	2.24	2.18
	Span 80	0.1	0.1	0.1	0.1
Phase II	Water	78.48	78.51	59.6	58.42
	Span 80	0.3	0.3	0.3	0.3

2.3. Characterization

Free films of nanocomposites were prepared by compression molding machine from ALEEY (Iran). Particle size (PS) of polymer particles were measured by a dynamic light scattering on a SEM 633 from SEMATech Co. (France) at fixed angle of light at 90° (at 25 °C) under laser beam (λ = 633 nm).

Films or powder was used for XRD measurement, recorded on a Siemens D5000 (Germany) using Cu Kα ray (λ = 1.54056 Å) as the radiation source, with a step size of 0.02° and a scan step time of 1 s. Where λ is the incident wavelength (1.54056 Å) and θ is the diffraction angle.

Small-angle X-ray scattering (SAXS) were performed by the Spanish CRG beam line BM16 in the European Synchrotron Radiation Facility in Grenoble (France). The monochromatic X-ray beam wavelength (λ) was 0.9795 nm with a sample-to-detector distance of 2.52 m. A 2-D detector mar CCD165 was used and the obtained two-dimensional scattering patterns were radically averaged using FIT2D program to obtain the scattered intensity ($I(q)$) profiles as a function of the scattering vector (q) calibrated to the diffraction peaks of silver-behenate.

TEM instrument model Tecnai G^2 from FEI Company (Netherland, Germany) at voltage of 200 kV was used which was kindly provided by the POLYMAT Institute. The samples were prepared by casting a drop of 40-50 times diluted latex solution onto a 200-mesh covered formvar/carbon coated copper grid at room temperature and dried at room and 60-80 °C overnight.

Minimum film formation temperature (MFFT) was made on a Pselecta instrument tester based on Standards: DIN-53787, DIN-53366, ASTM D-2354, ASTM D-1465, ISO-2115 and ISO/DIS-4622. Test instrument works with a ground hard-chrome metal plated as a measuring plate for depositing the latex. By heating and cooling the measuring plate, any variable temperature gradient within the range of -30 °C to +250 °C can be produced and kept constant for any given period as has been shown in Fig. 6. The measuring plate is equipped with 20 temperature sensors.

The temperature can be controlled by the integrated electronic temperature measuring instrument with a digital display and measuring-point selector over the entire range. For measuring the MFFT, latex is applied to the measuring plate by a film coating appliance [1, 21].

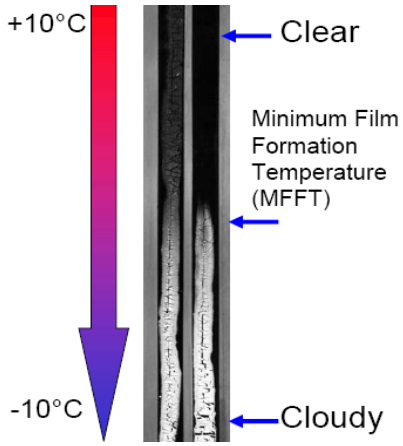

Fig. 6. Pselecta MFFT tester device [14].

Oxygen transmission rate (OTR) was tested by using Brugger (GDP-C) O_2-permeability tester (Munchen, Germany) according to ASTM D1434-82, method A.

The water vapor transmission rate (WVTR) data was measured by a computerized device. Latex free film was placed in the upper part of a cell containing a certain amount of water and then it was well-sealed so that water could only permeate through the free film. WVTR (g mm/cm^2 day) was calculated as follows:

$$WVTR = 8.64 \times 10^5 \times AB/[C(1-D)] \quad (1)$$

Where A, is the slope of the water vapor loss (g/s), B, is the thickness of the free film (mm), C, is the surface area of the free film (C = 2.54 cm^2), and D, is water vapor humidity [1, 21].

Water uptake of the latex films was measured according to the following procedure: dry films were weighed (m_1) and immersed in deionized water for 48 h. After storage in water, films were blot-dried and weighed again (m_2) [21, 23]. The water uptake was calculated by using the equation (Eq. 2) as follows: Water uptake (%) = $\frac{m_2 - m_1}{m_1} \times 100$ (2). The static contact angle for all of the free films' surfaces was measured by G2/G40 Kruss instrument (Germany) through sessile drop method using water droplet and average of 3 repeats.

3. Results and discussion

As was shown in Table 2, average particle size of nanocomposite latex with higher clay and solid contents was much bigger in comparison to the latex particles with small amounts of nanoclay.

Table 2. Particle size measured by DLS analysis.

Sample	Clay (wt%)	Solid content (%)	Average diameter (nm)
14 down	10	40	470
14 up	7	40	420
28 film powdered	10	20	350
28 film	7	20	290

Increase in the size of polymer particles should be another sign of encapsulation appeared through miniemulsion polymerization.

The SAXS profiles (the scattering intensity I (q), versus scattering vector, q) for 4 samples were shown in Fig. 7. At q = 1.6 nm^{-1} a peak appeared in the profiles of 14 down and 14 up which should be due to the not fully exfoliation of clay layers. This is attributed to high amount of clay or latex high solid content that inhibited formation of fully exfoliation structures.

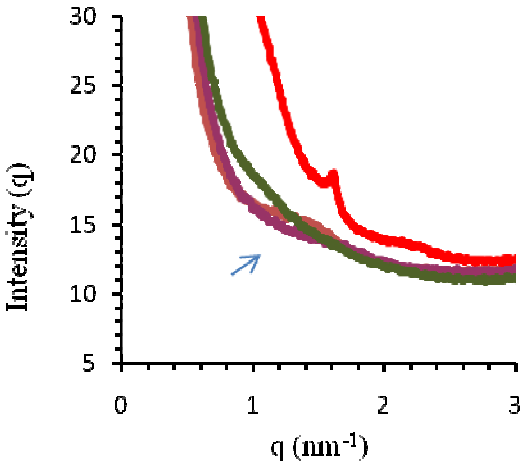

Fig. 7. SAXS: (brown) 14 up, (purple) 28 film powdered, (green) 28 film and (red) 14 down.

Cloisite 30B has an interlayer spacing of 1.74 nm which appeared as a sharp peak at 2θ ca. 5.08° in XRD pattern, as was shown in Fig. 8, XRD patterns of samples depict the disappearance of this sharp peak for 28 film powdered and 28 film but a small peak around 2θ = 4 to 6 explain that fully exfoliation of clay layers was not happened for 14 down and up samples.

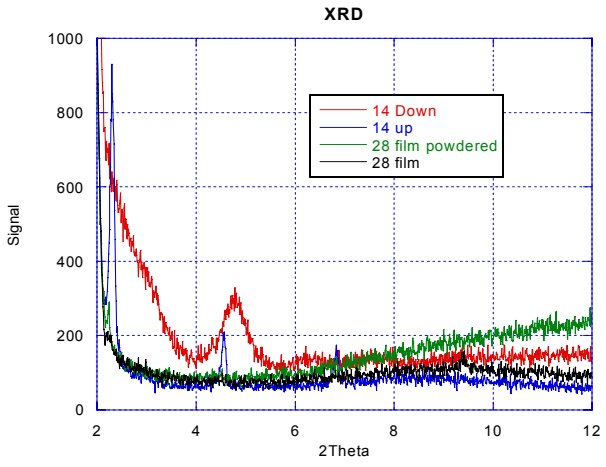

Fig. 8. XRD profiles for all 4 samples.

All these observations were also collected in Table 3.

Table 3. XRD and TEM observations.

Sample code	Encapsulation (TEM)	Exfoliation (XRD)
14 down	bad	limited
14 up	limited	limited
28 film powdered	good	fair
28 film	good	good

TEM micrographs were taken by dropping diluted latex on TEM copper grids. Some of them were dried at room temperature, and the others were heated about 60 °C. Figure 9 shows mono-size and spherical in shape polymer particles, in the range of 80 to 490 nm.

Some of Cloisite 30B particles were encapsulated within the polymer particles and some was located on the particles surfaces (Pickering). Figure 9 also shows stretched lines which were distributed individually all around the polymer film. These lines (stretched and separated) are clay platelets, which were exfoliated and well dispersed throughout the nanocomposite film.

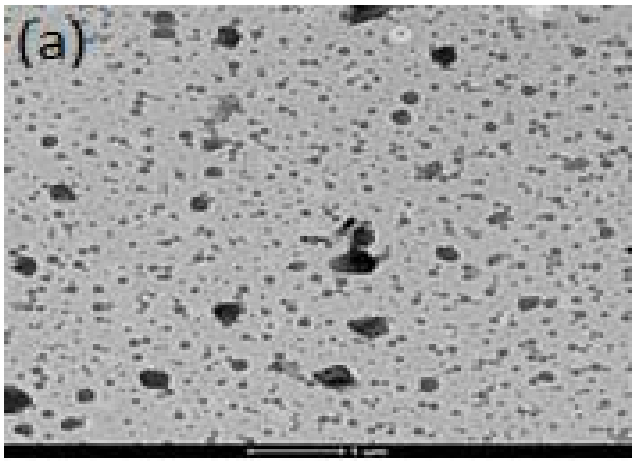

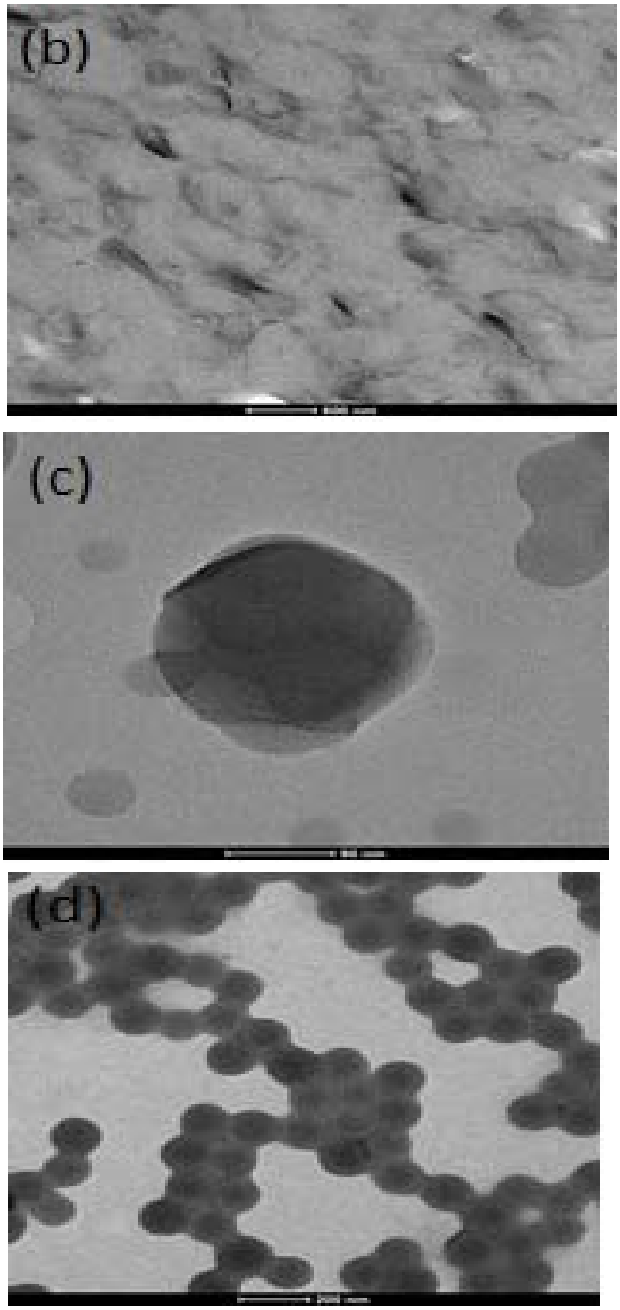

Fig. 9. TEM micrographs for all: (a) 14 down, (b) 14 up (c) 28 film powdered and (d) 28 film.

By increasing the clay content up to 10 wt%, both WVTR and OTR decreased compared to sample containing 7 wt% clay. On the other hand, degree of exfoliation has been decreased [1, 21].

Table 4. Permeability results for analyzed samples.

Sample Code	WVTR (gmm/cm^2 d)	OTR (cm^3/m^2 24h)	Water-up take (%)
14 down	12	500	3.8
14 up	8.9	250	3.3
28 film powdered	8.3	200	2.8
28 film	9.6	300	2.2

As we know, no mathematical relation was found between water and gas permeability. About water permeability, the interactions especially hydrogen bonding between water molecules and polymer chains are predominant, while for gases the diffusion process is so important [24-27].

By increasing the clay content and latex solid content, increase in water absorbency was found. Maybe degree of exfoliation or dispersion of clay has been decreased. On the other hand this kind of clay has hydrophilic properties, so if is not located in the form of encapsulated, may cause inverse effect on water absorbency.

Table 5. MFFT and contact angle results.

Sample Code	Θ (°C)	MFFT(°C)
14 down	96	38.7
14 up	98	37.5
28 film powdered	100.1	37.1
28 film	99	36.6

Also from contact angle results can deduce that by increasing the clay content, exfoliation degree was decreased and these particles could not encapsulated or located on the polymer particles as armored (Pickering) latex. Therefore, most of them had been dispersed in the matrix without any distinguished morphology. Contact angle and water absorbency increased except for sample 28 film which showed more encapsulation degree of clay layers within polymer particles.

4. Conclusion

Researchers proved that reduction in permeability is due to the clay content; exfoliation of clay layers and its dispersion within matrix against diffusion of permeate. In this work, due to the high solid content and clay amounts, various morphologies were observed, for example some clay particles appeared on the surface of polymer particles.

This is similar to the principle of Pickering (armored) emulsion polymerization in which the whole system is stabilized by solid particles (here is clay) and not by surfactant. Observed armored latex particles suggest new barrier applications with honeycomb morphology. This honeycomb structure is suitable for making barrier packaging film against water and gases.

Acknowledgment

The financial support of this work by Iran Polymer and Petrochemical Institute (IPPI, Iran-Tehran) and POLYMAT Institute of the University of the Basque Country- Spain (Prof. J. R. Leiza and Prof. Chema Asua) is gratefully acknowledged. Also assistance of Mr Shahram khamisabadi is appreciated.

References

[1]. G. Diaconu, Production of waterborne polymer/clay nanocomposite, Universidad del Pais Vasco, POLYMAT, Spain, Ph.D. thesis, 2008.

[2]. M. Alexandre, P. Dubois, Mat. Sci. Eng., 28 (1-2) (2000) 1-63.

[3]. A. Blumstein, Bull. Chem. Soc. 1 (1961) 899-904.

[4]. Z. Tong, Water-based suspension of polymer nanocomposite prepared via miniemulsion polymerization, Georgia Institute of Technology, USA, Ph.D. thesis, 2007.

[5]. A. Usuki, M. Kawasumi, Y. Kojima, A. Okada, T. Kurauchi, O. Kamigaito, J. Mater. Res. 8(5) (1993) 1174-1178.

[6]. G. Choudalakis, A. D. Gotsis, European Polymer Journal 45 (2009) 967-984.

[7]. K. Yano, A. Usuki, and A. Okada, J. Polym. Sci., Part A, Polym. Sci. Chem. 35 (1997) 2289-2295.

[8]. P. B. Messersmith and E. P.Giannelis, J. Polym. Sci. Part A, Polym. Chem. 33 (7) (1995) 1047-1057.

[9]. M. Antoniettie, K. Landfester, Prog. Polym. Sci., 27(4) (2002) 689-757.

[10]. K. Landfester, Macromol. Rapid. Commun. 22 (2001) 896-936.

[11]. S. K. (Ed.) Ghosh, Functional Coatings by polymer microencapsulation, WILEY-CH Verlag GmbH & Co. KGaA, Weinheim, 2006.

[12]. J. V. Koleske, Encyclopedia of Analytical Chemistry, Meyers R. A. (Ed.), John Wiley & Sons Ltd., Chichester, Chapter 4, 2000.

[13]. A. D. Wilson, J. W. Nicholson, H. J. Prosser, Surface Coatings-1, Elsevier Applied Science, New York, Chapter 1, 1987.

[14]. J. L. Keddie, Emulsion Polymerization Process Course, Polymat, Spain, 2008, 2009.

[15]. E. T. a. van den Dungen, J. Galineau, and P. C. Hartmann, Macromolecular Symposia, 313–314(1) (2012) 128–134.

[16]. A. Bonnefond, M. Paulis, S. A. F. S. Bon, and J. J. R. Leiza, Langmuir, 29(7) (2013) 2397–2405.

[17]. R. Ianchis, L. O. Cinteza, D. Donescu, C. Petcu, M. C. Corobea, R. Somoghi, M. Ghiurea, and C. Spataru, Applied Clay Science 52(1–2) (2011) 96–103.

[18]. N. Greesh, R. Sanderson, and P. Hartmann, Polymer 53(3) (2012) 708–718.

[19]. L. Hatami, V. Haddadi-Asl, H. R. Mamaqani, L. Ahmadian-Alam, M. S. Kalajahi, Polymer Composites 32(6) (2011) 967–975.

[20]. K. Khezri, V. Haddadi-Asl, H. R. Mamaqani, M. S. Kalajahi, Polymer Engineering 32(2) (2012) 111–119.

[21]. M. Mirzataheri, Acrylic-Based Nanocomposite Barrier Coatings Including Nanoclay Prepared via Miniemulsion Polymerization, ph.d. Thesis, IPPI, Iran 2009.

[22]. N. N. Herrera, S. Persoz, J. L. Putaux, L. David, E. Bourgeat-Lami, Journal of Nanoscience and Nanotechnology 6(2) (2006) 421-431.

[23]. N. Salahuddin, Polymer Composites, 30(1) (2009) 13-21.

[24]. K. M. (Eds.) Finlayson, Plastic film technology, high barrier plasticfilms for packaging, Vol. 1, Technomic Pub. Company, Lancaster, 1989.

[25]. M. Mirzataheri, A.R. Mahdavian M. Atai, Colloid. Polym. Sci. 287 (2009) 725-732.

[26]. M. Mirzataheri, M. Atai, A.R. Mahdavian, J. Polymer Sci. 118 (2010) 3284-3291.

[27]. M. Mirzataheri, A.R. Mahdavian M. Atai, Polym. Int. 60 (2011) 613-619.